

INtra-Procedural UltraSound Imaging for DEtermination of Atrial Wall Thickness and Acute Tissue Changes After Isolation of the Pulmonary Veins with Radiofrequency, Cryoballoon or Laser Balloon Energy: the INSIDE PVs Study

Milena Leo (✉ milena.leo@ouh.nhs.uk)

Oxford University Hospitals NHS Trust: Oxford University Hospitals NHS Foundation Trust
<https://orcid.org/0000-0001-6991-6664>

Giovanni Luigi De Maria

Oxford University Hospitals NHS Trust: Oxford University Hospitals NHS Foundation Trust

Andre Briosca e Gala

Oxford University Hospitals NHS Trust: Oxford University Hospitals NHS Foundation Trust

Michael Pope

Oxford University Hospitals NHS Trust: Oxford University Hospitals NHS Foundation Trust

Abhirup Banerjee

University of Oxford

Andrew Kelion

Oxford University Hospitals NHS Trust: Oxford University Hospitals NHS Foundation Trust

Michala Pedersen

Oxford University Hospitals NHS Trust: Oxford University Hospitals NHS Foundation Trust

Kim Rajappan

Oxford University Hospitals NHS Trust: Oxford University Hospitals NHS Foundation Trust

Matthew Ginks

Oxford University Hospitals NHS Trust: Oxford University Hospitals NHS Foundation Trust

Yaver Bashir

Oxford University Hospitals NHS Trust: Oxford University Hospitals NHS Foundation Trust

Ross J Hunter

Barts and The London School of Medicine and Dentistry William Harvey Research Institute

Tim R Betts

University of Oxford

Keywords: intracardiac echocardiography, intravascular ultrasound, left atrial wall thickness, acute wall changes after ablation, radiofrequency energy, cryoenergy, laser energy.

Posted Date: June 23rd, 2021

DOI: <https://doi.org/10.21203/rs.3.rs-637740/v1>

License: © ⓘ This work is licensed under a Creative Commons Attribution 4.0 International License.

[Read Full License](#)

Version of Record: A version of this preprint was published at The International Journal of Cardiovascular Imaging on September 23rd, 2021. See the published version at <https://doi.org/10.1007/s10554-021-02417-7>.

Abstract

Introduction

Preliminary data in human suggest that both Intracardiac echocardiography (ICE) and Intravascular ultrasound (IVUS) can be used for real-time information on the left atrial (LA) wall thickness and on the acute tissue changes produced by energy delivery. This pilot study was conducted to compare ICE and IVUS for real-time LA wall imaging and assessment of acute tissue changes produced by radiofrequency (RF), cryo and laser catheter ablation.

Methods

Patients scheduled for RF, cryoballoon or laser balloon Pulmonary Vein Isolation (PVI) catheter ablation were enrolled. Each pulmonary vein (PV) was imaged immediately before and after ablation with either ICE or IVUS. The performance of ICE and IVUS for imaging were compared. Pre- and post-ablation measurements (lumen and vessel diameters, areas and sphericity indexes, wall thickness and muscular sleeve thickness) were taken at the level of each PV ostium.

Results

A total of 48 PVs in 12 patients were imaged before and after ablation. Compared to IVUS, ICE showed higher imaging quality and inter-observer reproducibility of the PV measurements obtained. Acute wall thickening suggestive of oedema was observed after RF treatment ($p = 0.003$) and laser treatment ($p = 0.003$) but not after cryoablation ($p = 0.69$).

Conclusions

Our pilot study suggests that ICE is preferable to IVUS for LA wall thickness imaging at the LA-PV junctions during ablation. Ablation causes acute wall thickening when using RF or laser energy, but not cryoenergy delivery. Larger studies are needed to confirm these preliminary findings.

Introduction

One of the major limitations of percutaneous catheter ablation is the inability to image the cardiac tissue thus providing real-time information on wall thickness and on acute tissue changes produced by energy delivery during ablation. Due to the unpredictable variability of the wall thickness in the areas targeted for ablation^{1,2}, choosing appropriate ablation settings for creation of effective lesions is often challenging. Insufficient ablation will translate into non-transmural and non-durable lesions, while excessive ablation could lead to steam pops, cardiac perforation and damage to surrounding anatomical structures (e.g. the esophagus). Moreover, very little is known about acute tissue changes produced by catheter ablation and the role they might play in lesion failure. Acute development of tissue oedema has been reported when using radiofrequency (RF) energy for ablation³⁻⁵ and it has been advocated as a

possible mechanism accounting for lesion failure^{6,7}. The presence and degree of acute tissue oedema when using cryoenergy or laser energy for ablation is not known.

Ultrasound imaging has previously been used in animal studies for assessment of atrial wall thickness and lesion formation during catheter ablation⁸⁻¹⁰. Preliminary data in human also suggest that ultrasound imaging modalities such as intracardiac echocardiography (ICE) and intravascular ultrasound (IVUS) can be used for left atrial (LA) wall thickness measurements and detection of acute changes produced by ablation¹¹⁻¹³.

This pilot study was conducted to compare ICE and IVUS for real-time LA wall imaging and assessment of acute tissue changes produced by different ablation energies during pulmonary vein isolation (PVI).

Methods

Study design

The INSIDE PVs study (INtra-procedural ultraSound Imaging for DEtermination of atrial wall thickness and acute tissue changes after isolation of the Pulmonary Veins with radiofrequency, cryoballoon or laserballoon energy) was a single-center prospective pilot study. The trial was approved by the Local Ethics Committee, complied with the Declaration of Helsinki and was registered on www.clinicaltrials.gov (Identifier NCT03372798).

Patients scheduled for RF, cryoballoon or laserballoon PVI catheter ablation for symptomatic, drug-refractory paroxysmal atrial fibrillation (AF) were eligible for the trial. All AF ablations were performed in a standard fashion, as described in the supplementary section.

Protocol for ICE/IVUS imaging of the PVs

As part of the trial, ultrasound imaging of the junctions between LA and pulmonary veins (PVs) was performed with either ICE or IVUS as per operator's discretion.

For ICE imaging, a 9F catheter with a 9 MHz rotational transducer providing a maximal radial depth of 50 mm (Ultra ICE, Boston Scientific) was used. For IVUS imaging, a 20 MHz digital probe with maximum ultrasonic detection depth of 24 mm (Visions PV .018, Volcano, San Diego, CA) was chosen and used mounted on a guidewire (0.014-in percutaneous transluminal coronary angioplasty guidewire) as per manufacture instructions.

The ultrasound-imaging probe was introduced into the LA via the trans-septal access and advanced under fluoroscopic guidance distally into each pulmonary vein (PV) with the aid of a long steerable sheath. Images were recorded during slow manual pullback of the probe from each vein into the LA body. Each PV was imaged twice, before and after ablation.

Offline ICE/IVUS quantitative images analysis

Images were stored and analyzed offline by two independent operators, blinded to clinical and procedural data, at the OxACCT CoreLab (Oxford Academic Cardiovascular CT CoreLab) using QIVUS software (Medis Medical, Leiden, The Netherlands). Images analysis was performed as previously outlined^{14,15}.

Lumen and vessel diameters, areas and sphericity indexes and wall thickness were measured at the level of the PV ostium as indicated in Figure 1. The PV ostium was identified as point of maximal inflection between LA and PV wall, as previously described¹⁶.

Comparisons between corresponding PV measurements obtained from ICE and IVUS frames and between pre- and post-ablation measurements were made. Post-ablation morphological changes of the PV wall such as dissection-like changes were recorded.

Assessment of performance of ICE and IVUS

The time required for imaging and any procedural complications associated with imaging were recorded as indicators of trackability of ICE and IVUS catheters.

The imaging quality of each PV cross-section was defined as good, satisfactory, sub-optimal and poor: good quality if the vessel contour was visible in all 4 quadrants; satisfactory quality if the vessel contour was visible in 3 quadrants; sub-optimal quality if the vessel contour was visible in 2 non-consecutive quadrants; poor quality if not possible to define the vessel contour as visible only in one quadrant or in two consecutive quadrants (Figure 2). Poor quality images were discarded and not considered for quantitative analyses.

The inter-observer agreement for quantitative data was also assessed for both ICE and IVUS by calculating intraclass correlation coefficient (ICC) values for different PV measurements.

Follow-up data

Although the study was not designed to assess and compare clinical outcomes, long-term data were obtained from standard clinical follow-up appointments. The need of redo catheter ablation due to recurrence of atrial tachyarrhythmias and which PVs were found to be reconnected at the redo procedure were reported.

Statistical analysis

Categorical variables were expressed as absolute number and percentage (%). Continuous variables were expressed as mean and (\pm) standard deviation (SD) or as median accompanied by interquartile range (IQR), as appropriate after checking for normality using the Shapiro-Wilk's test. Categorical variables were compared with the use of the Pearson's Chi-square test or Fisher's exact test, as appropriate. Continuous variables were compared with the use of one-way ANOVA test or Kruskal-Wallis test, as appropriate according to data distribution.

A two-sided P value of less than 0.05 was considered to indicate statistical significance. Data were analysed with the use of SPSS software version 27 (IBM Statistics, Chicago, Illinois).

Results

Study population

Twelve patients undergoing PVI catheter ablation for paroxysmal AF were enrolled. The patients' baseline characteristics are presented in Table A of the Supplementary Section.

Pulmonary vein isolation was performed with RF in 5 patients (20 PVs), with cryoballoon in 4 patients (16 PVs) and with laserballoon in 3 patients (12 PVs). All 48 PVs were isolated. A total of 28 PVs in 7 patients were imaged before and after PVI with ICE, while 20 veins in 5 patients were imaged with IVUS.

Performance of ICE/IVUS for PV imaging

No significant differences in terms of trackability were observed between ICE and IVUS catheters (additional procedural time required for imaging: ICE = 24.8 ± 3.4 min, IVUS = 25 ± 3.5 min, $p = 0.95$; no procedural complications).

As shown in Table 1, ICE produced higher imaging quality than IVUS ($\chi^2 = 35.415$; $p < 0.001$).

Compared to IVUS, ICE also performed better in terms of inter-observer reproducibility of PV measurements, as showed in Table B of the supplementary section. Although both techniques showed excellent ICC values for PV lumen measurements, IVUS showed only moderate ICC values for PV vessel and wall thickness measurements, as compared to good and excellent ICC values exhibited by ICE for corresponding measurements.

ICE/IVUS images analysis

Out of the 48 PV cross-sections, 3 were discarded because of poor quality and 45 (28 ICE and 17 IVUS frames) were considered adequate for quantitative analysis.

Compared to the IVUS cross-sections, the ICE ones showed larger lumen and vessel diameters and areas, larger wall thicknesses and significantly lower lumen and vessel sphericity indexes, indicative of more oval/elliptical shape of both lumen and vessel contours (Table 2). Of note, median pre- and post-ablation wall thickness index percentage (WTI%) and muscular sleeve thicknesses did not differ between ICE and IVUS-imaged PVs.

As detailed in Table 3, statistically significant increases of mean wall thickness, wall thickness index (WTI) and WTI%, suggestive of acute wall thickening, were observed after ablation in both ICE and IVUS cross-sections. A significant reduction of the thickness of the muscular sleeve was also observed after ablation [ICE cross-sections: median (IQR) percentage reduction = 8.2 ($0-45.9$)%; IVUS cross-sections:

median (IQR) percentage reduction= 31.68 (14.54-81.64)%, with complete disappearance of the muscular sleeve after ablation in 6 PVs out of 45.

When grouping by ablation technology used for PVI (RF, cryo or laser), the increase in WTI% was observed only after RF treatment ($p = 0.003$) and laser treatment ($p = 0.003$), whilst no significant changes in wall thickness were observed after cryoablation ($p = 0.69$) (Figure 3, Table 4).

A single case of vessel dissection was documented after ablation (right inferior pulmonary vein after cryoballoon ablation) (Figure 4).

Follow-up data

Patients were followed up for 26.5 ± 4.1 months. Six patients (50%) required a redo procedure due to recurrence of atrial tachyarrhythmias 3 months or later after the AF ablation. Of them, 67% (4 patients) had reconnected PVs, for a total of 7 reconnected PVs out of the 24 checked during the redo procedures.

Reconnected and isolated PVs at the second ablation procedure showed similar degrees of wall thickness increase [median (IQR) WTI% increase: reconnected PVs = 5.71 (0.31-12.04) %; isolated PVs: = 4.51 (0.94-12.07) %; $p = 0.89$] and muscular sleeve thickness reduction after the first ablation procedure [median (IQR) percentage reduction: reconnected PVs= 8.72 (0.3- 44.5) %; isolated PVs=24.53 (0.5- 41.18) %; $p = 0.58$].

Discussion

Our pilot study was conducted to compare ICE and IVUS for real-time LA wall imaging and for detection of acute tissue changes produced by different ablation energies during PVI catheter ablation. Although both ICE and IVUS probes image in the axial plan, providing cross-sectional images of the vessel (or chamber of interest) and surrounding tissues, their transducers use different ranges of ultrasound frequencies. The catheter designs are also different: the IVUS catheter has a smaller size (6F) and uses a mono-rail system, with the distal portion of the catheter advanced over a guidewire for better support and stability, while the ICE catheter has a bigger size (9F) and no central lumen. We chose to compare a 9MHz ICE catheter with a 20MHz IVUS probe to investigate which ultrasound frequency would give the best compromise between contrast resolution and image penetration for PVs imaging.

Performance of ICE and IVUS

In our study, ICE performed better than IVUS with regards to quality of imaging provided and to inter-observer reproducibility of measurements obtained. These findings are likely due to the lower ultrasound frequency used by ICE, which was advantageous in terms of acoustic penetration without a significant loss in spatial resolution. When using ICE, the outer vessel circumference was well-defined in most or all image quadrants, as well as inner structures such as lumen circumference and wall.

We observed no significant differences between the two technologies in terms of trackability: similar additional procedural times were needed for ICE and for IVUS imaging and no procedural complications occurred as result of imaging.

Both lumen and vessel diameters and areas were consistently larger in the ICE-imaged PVs compared to the IVUS-imaged PVs. Moreover, although both imaging techniques showed an elliptical shape of the PV cross-sections, in keeping with previous CT and MRI studies^{17,18}, lumen and vessel sphericity indexes were lower in the ICE-imaged PVs, which is indicative of a more elliptical shape of the PV cross-sections. Our PV measurements determined by IVUS are in line with previously reported PV measurements, obtained from both IVUS images and histological sections¹⁵. Taken together, these data might suggest that ICE overestimated the PVs sizes due to non-coaxial cross-sectioning, as indicated by the lower sphericity index when compared to the IVUS images. ICE catheters are not advanced or pulled back over a wire and this different design might have reduced the chance of a coaxial position of the probe within the PV lumen. Despite different lumen and vessel diameters and absolute areas, pre- and post-ablation WTI% were comparable between PV cross-sections imaged either ICE or IVUS, thus suggesting that both imaging modalities can provide similar accuracy in depicting acute changes in tissue thickness after ablation.

Acute changes produced by the different ablation energies

In our study, the LA wall thickness was found to increase similarly at the level the PV ostia following ablation when using RF or laser balloon energy, while no increase in wall thickness was observed when using the cryoballoon. While acute development of tissue oedema is well known after RF,^{9,19,20} limited data are available regarding acute tissue changes after laser energy delivery^{13,21,22}. Apart from the lack of direct contact of the energy source with the tissue (the optical fiber delivering arc of laser energy is in a balloon), laser energy as with RF produces tissue damage through heating and is delivered in a point-by-point fashion. Thus, it is not surprising that the two energy modalities might share similar mechanisms of tissue injury, including acute wall thickness increase from oedema. In the study by Mangrum et al¹³, a significantly more pronounced wall thickening was observed after RF ablation than after laser ablation, however a lower RF power was used.

In another IVUS study¹¹, tissue oedema was reported in 90% of the PVs after cryoablation (and similar number of freezes per vein). Of note, in this study dissection-like changes were also observed, together with oedema, in most of the PVs, while in our study dissection-like changes were observed only in one vein after cryoballoon ablation and, interestingly, this occurred in the context of acute wall tissue thickening. It could be hypothesized that in these veins the oedema was due to the mechanical injury associated with dissection, rather than being a direct consequence of cryoenergy delivery. In the sequential process of tissue injury produced by cryoenergy^{23,24}, tissue oedema is thought to occur only at a late stage, once the tissue has thawed, following freezing, and has become hyperaemic, and to gradually progress over subsequent hours²⁵. Concordantly, early PV imaging in our study showed no acute wall thickening suggestive of development of oedema.

The different morphological changes produced by the different ablation energies could suggest different mechanisms of lesion failure. Recent data suggest that the adjustment of the ablation settings based on baseline LA wall thickness can improve the procedure outcome and reduce the risk of collateral injury¹². A further adjustment based on the acute wall thickening produced by energy delivery for ablation could also be beneficial when using RF or laser energy and could potentially highlight gaps between lesions.

Apart from acute wall thickening, we observed a reduction of the thickness of the PV muscular sleeve after PVI catheter ablation. Myocardial sleeves are known to extend from the left atrium into the PVs walls and to be a source of focal activity triggering AF²⁶. The thickness reduction after ablation could indicate damage, translating to elimination of the PV potentials and acute electrical isolation of the vein and may also explain why it is often impossible to get local capture during pacing to demonstrate exit-block. Whether durable PV isolation correlates with a certain degree of wall thickness reduction or complete disappearance of the muscular sleeve after catheter ablation is unclear. We did not observe a correlation between degree of wall thickness increase or muscular sleeve thickness reduction after the first catheter ablation procedure and evidence of PV reconnection at the second catheter ablation procedure, however only a small number of PVs were checked with a second ablation procedure in our study.

Limitations

There are some limitations in our work that must be acknowledged. First, results need to be interpreted as hypothesis-generating and in light of the small and heterogeneous sample size, due to the use of different imaging modalities and different ablation modalities.

No direct comparisons between ICE and IVUS were made by imaging the same PVs with both modalities. No other imaging modality or histopathology were available as reference for the PVs measurements obtained with ICE and IVUS to ascertain which of the two imaging modalities gave more accurate measurements. However, this did not preclude confirming the feasibility of both ICE and IVUS for LA wall imaging, since comparable wall thickness measurements were obtained and similar acute changes in wall thickness were detected with both imaging modalities.

Pullback was manual rather than automatic. This precluded the precise comparison of distal cross-sections before and after ablation.

Imaging during energy delivery was not attempted as the same trans-septal access was used for either ablation catheter or imaging catheter. However, simultaneous imaging might not have been possible due to spatial interference, especially when using cryo or laser balloon catheters, and/or due to artifacts created by irrigation of the RF catheter.

Conclusions

In our pilot study, ICE performed better than IVUS with regards to imaging quality and inter-observer reproducibility of measurements obtained. Acute wall thickening was observed at the PV ostia after RF

and laser energy delivery and not after cryoenergy delivery. Larger studies are needed to confirm these preliminary findings.

Abbreviations

AF = atrial fibrillation; ICE = Intracardiac echocardiography; IQR = Interquartile range; IVUS= Intravascular ultrasound; LA = Left atrial; PV = Pulmonary vein; PVI = Pulmonary vein isolation; PVs = Pulmonary veins; RF= Radiofrequency; SD = Standard deviation; WTI = Wall thickness index; WTI%= Wall thickness index percentage.

Declarations

ACKNOWLEDGEMENTS

We thank the John Radcliffe Hospital Cardiac Angiography Suite Team and the Oxford Cardiac Research Team for their invaluable help and support for the conduction of the study.

FUNDING

This study was funded by a grant of the National Institute for Health Research (NIHR) Oxford Biomedical Research Centre. Prof. Betts is supported by the Oxford NIHR Biomedical Research Centre. Dr Leo's salary was supported by an unrestricted research grant from Abbott Medical.

CONFLICT OF INTERESTS STATEMENTS

Dr Ginks has received speaker's fees from Abbott and Biosense Webster.

Dr Rajappan has received speaker's fees from Abbott.

Dr Hunter has received research grants, educational grants and speaker's fees from Biosense Webster and Medtronic; he is an inventor of the STAR Mapping system and shareholder in Rhythm AI Ltd.

Dr Betts has received research funding, speaker's fees and advisory board fees from Abbott. The other authors have no conflict of interests to declare.

DATA AVAILABILITY

The data that support the findings of this study are available from the corresponding author upon reasonable request.

CONSENT TO PARTICIPATE

All patients provided informed consent for participation in the INSIDE PVs study.

CONSENT FOR PUBLICATION

All patients provided informed consent for anonymous publication of the results of the study.

ETHICAL APPROVAL

The INSIDE PVs study was approved by the Health Research Authority West Midlands Coventry and Warwickshire Research Ethics committee and conducted in accordance with the Declaration of Helsinki (REC number 16/WM/0379).

AUTHOR CONTRIBUTIONS

All authors contributed to the study conception and design. Material preparation, data collection and analysis were performed by Milena Leo and Giovanni Luigi De Maria. The first draft of the manuscript was written by Milena Leo and all authors commented on previous versions of the manuscript. All authors read and approved the final manuscript.

References

1. Hall B, Jeevanantham V, Simon R, Filippone J, Vorobiof G, Daubert J (2006) Variation in left atrial transmural wall thickness at sites commonly targeted for ablation of atrial fibrillation. *J Interv Card Electrophysiol* 17:127–132
2. Ho SY, Sanchez-Quintana D, Cabrera JA, Anderson RH (1999) Anatomy of the left atrium: implications for radiofrequency ablation of atrial fibrillation. *J Cardiovasc Electrophys* 10:1525–1533
3. Schwartzman D, Ren JF, Devine WA, Callans DJ (2001) Cardiac swelling associated with linear radiofrequency ablation in the atrium. *J Interv Card Electrophysiol* 5:159–166
4. Weerasooriya R, Jaïs P, Sanders P et al (2003) Images in cardiovascular medicine. Early appearance of an edematous tissue reaction during left atrial linear ablation using intracardiac echo imaging. *Circulation* 108:e80
5. Okada T, Yamada T, Murakami Y et al (2007) Prevalence and Severity of Left Atrial Edema Detected by Electron Beam Tomography Early After Pulmonary Vein Ablation. *J Am Coll Cardiol* 49:1436–1442
6. Yamada T, Murakami Y, Okada T et al. Incidence, location, and cause of recovery of electrical connections between the pulmonary veins and the left atrium after pulmonary vein isolation. *Europace: European pacing, arrhythmias, and cardiac electrophysiology : journal of the working groups on cardiac pacing, arrhythmias, and cardiac cellular electrophysiology of the European Society of Cardiology* 2006;8:182–8
7. Arujuna A, Karim R, Caulfield D et al (2012) Acute pulmonary vein isolation is achieved by a combination of reversible and irreversible atrial injury after catheter ablation: evidence from magnetic resonance imaging. *Circulation Arrhythmia electrophysiology* 5:691–700

8. Ren JF, Callans DJ, Schwartzman D, Michele JJ, Marchlinski FE (2001) Changes in local wall thickness correlate with pathologic lesion size following radiofrequency catheter ablation: an intracardiac echocardiographic imaging study. *Echocardiography* 18:503–507
9. Granier M, Winum PF, Granier M et al (2015) Real-time atrial wall imaging during radiofrequency ablation in a porcine model. *Heart rhythm* 12:1827–1835
10. Ren JF, Callans DJ, Schwartzman D, Michele JJ, Marchlinski FE (2001) Changes in local wall thickness correlate with pathologic lesion size following radiofrequency catheter ablation: an intracardiac echocardiographic imaging study. *Echocardiography* 18:503–507
11. Baran J, Lewandowski P, Smarż K, Sikorska A, Zaborska B, Kułakowski P. Acute Hemodynamic and Tissue Effects of Cryoballoon Ablation on Pulmonary Vessels: The IVUS-Cryo Study. *J Am Heart Assoc* 2017;6
12. Motoike Y, Harada M, Ito T et al. Wall Thickness-Based Adjustment of Ablation Index Improves Efficacy of Pulmonary Vein Isolation in Atrial Fibrillation: Real-Time Assessment by Intracardiac Echocardiography. *Journal of cardiovascular electrophysiology* 2021
13. Gao XA-O, Chang DA-O, Bilchick KC et al (2021) Left atrial thickness and acute thermal injury in patients undergoing ablation for atrial fibrillation: Laser versus radiofrequency energies. *J Cardiovasc Electrophys* 32:1259–1267
14. Mintz GS, Nissen SE, Anderson WD et al (2001) American College of Cardiology Clinical Expert Consensus Document on Standards for Acquisition, Measurement and Reporting of Intravascular Ultrasound Studies (IVUS). A report of the American College of Cardiology Task Force on Clinical Expert Consensus Documents. *J Am Coll Cardiol* 37:1478–1492
15. Cabrera JA, Sánchez-Quintana D, Farré J et al (2002) Ultrasonic characterization of the pulmonary venous wall: echographic and histological correlation. *Circulation* 106:968–973
16. Ang R, Hunter RJ, Baker V et al (2015) Pulmonary vein measurements on pre-procedural CT/MR imaging can predict difficult pulmonary vein isolation and phrenic nerve injury during cryoballoon ablation for paroxysmal atrial fibrillation. *Int J Cardiol* 195:253–258
17. Jongbloed MR, Bax JJ, Lamb HJ et al (2005) Multislice computed tomography versus intracardiac echocardiography to evaluate the pulmonary veins before radiofrequency catheter ablation of atrial fibrillation: a head-to-head comparison. *J Am Coll Cardiol* 45:343–350
18. Wittkampf FH, Vonken EJ, Derksen R et al (2003) Pulmonary vein ostium geometry: analysis by magnetic resonance angiography. *Circulation* 107:21–23
19. Haines DE, Wright M, Harks E et al. Near-Field Ultrasound Imaging During Radiofrequency Catheter Ablation: Tissue Thickness and Epicardial Wall Visualization and Assessment of Radiofrequency Ablation Lesion Formation and Depth. *Circulation Arrhythmia and electrophysiology* 2017;10
20. Wright M, Harks E, Deladi S et al (2018) Characteristics of Radiofrequency Catheter Ablation Lesion Formation in Real Time In Vivo Using Near Field Ultrasound Imaging. *JACC Clinical electrophysiology* 4:1062–1072

21. Reddy VY, Neuzil P, Themistoclakis S et al (2009) Visually-guided balloon catheter ablation of atrial fibrillation: experimental feasibility and first-in-human multicenter clinical outcome. *Circulation* 120:12–20
22. Gerstenfeld EP, Michele J (2010) Pulmonary vein isolation using a compliant endoscopic laser balloon ablation system in a swine model. *J Interv Card Electrophysiol* 29:1–9
23. Khairy P, Dubuc M (2008) Transcatheter cryoablation part I: preclinical experience. *Pacing clinical electrophysiology: PACE* 31:112–120
24. Lustgarten DL, Keane D, Ruskin J (1999) Cryothermal ablation: mechanism of tissue injury and current experience in the treatment of tachyarrhythmias. *Prog Cardiovasc Dis* 41:481–498
25. Gage AA, Baust J (1998) Mechanisms of tissue injury in cryosurgery. *Cryobiology* 37:171–186
26. de Bakker JM, Ho Sy Fau - Hocini M, Hocini M (2002) Basic and clinical electrophysiology of pulmonary vein ectopy. *Cardiovasc Res* 54:287–294

Tables

Table 1. Imaging quality: comparison between ICE and IVUS.

	ICE	IVUS
Image Quality , number of PV runs (%)		
Good	24 (86%)	0 (0%)
Satisfactory	4 (14%)	13 (65%)
Sub-optimal	0 (0%)	4 (20%)
Poor	0 (0%)	3 (15%)
Total	28	20

Table 2. Comparison between corresponding PV measurements obtained with ICE and IVUS.

	ICE imaging	IVUS imaging	p
PRE-ABLATION			
Mean lumen diameter (mm),mean ± SD	18.57 ± 3.77	10.96 ± 2.24	< 0.0001
Maximum lumen diameter (mm),mean ± SD	22.23 ± 4.85	12.2 ± 2.76	< 0.0001
Minimum lumen diameter (mm),mean ± SD	15.69 ± 3.58	9.89 ± 2.09	< 0.0001
Lumen sphericity index, mean ± SD	0.72 ± 0.14	0.82 ± 0.11	0.012
Lumen area (mm ²), mean ± SD	281.46 ± 115.06	98.05 ± 36.74	< 0.0001
Mean vessel diameter (mm),mean ± SD	21.21 ± 3.72	12.58 ± 2.5	< 0.0001
Maximum vessel diameter (mm),mean ± SD	24.57 ± 4.78	13.61 ± 2.90	< 0.0001
Minimum vessel diameter (mm), mean ± SD	18.36 ± 3.50	11.69 ± 2.42	< 0.0001
Vessel sphericity index, mean ± SD	0.76 ± 0.13	0.87 ± 0.09	0.005
Vessel area (mm ²), mean ± SD	363.84 ± 130.33	129.02 ± 47.34	< 0.0001
Muscular sleeve thickness (mm),median (IQR)	0.55 (0.34- 0.70)	0.35 (0.11-0.60)	0.12
Mean wall thickness (mm), median (IQR)	1.18 (0.95-1.52)	0.78 (0.67-0.84)	< 0.0001
Maximum wall thickness (mm), median (IQR)	2.02 (1.62-3.03)	1.36 (1.09-1.52)	< 0.0001
Minimum wall thickness (mm), median (IQR)	0.41 (0.25-0.63)	0.26 (0.22-0.32)	0.04
WTI (mm ²), median (IQR)	73.39 (55.79-109.5)	29.67 (24.4-33.9)	< 0.0001
WTI% (%),median (IQR)	22.18 (16.4-29.1)	23.15 (20.8-27.8)	0.51
POST-ABLATION			
Mean lumen diameter (mm), mean ± SD	18.3 ± 3.97	10.93 ± 2.16	< 0.0001
Maximum lumen diameter (mm), mean ± SD	22.45 ± 4.82	12.29 ± 2.41	< 0.0001
Minimum lumen diameter (mm), mean ±	14.75 ± 4.27	9.85 ± 2.21	<

SD			0.0001
Lumen sphericity index , mean ± SD	0.66 ± 0.13	0.81 ± 0.12	0.004
Lumen area (mm²) , mean ± SD	275.48 ± 118.24	97.36 ± 34.64	< 0.0001
Mean vessel diameter (mm) , mean ± SD	21.54 ± 3.94	12.95 ± 2.39	< 0.0001
Maximum vessel diameter (mm) , mean ± SD	25.18 ± 5.1	14.06 ± 2.72	< 0.0001
Minimum vessel diameter (mm) , mean ± SD	18.36 ± 3.53	11.99 ± 2.37	< 0.0001
Vessel sphericity index , mean ± SD	0.74 ± 0.13	0.86 ± 0.1	0.003
Vessel area (mm²) , mean ± SD	374.56 ± 139.38	136.00 ± 46.33	< 0.0001
Muscular sleeve thickness (mm) ,median (IQR)	0.37 (0.33-0.51)	0.22 (0.01-0.46)	0.39
Mean wall thickness (mm) ,median (IQR)	1.52 (1.20-1.90)	0.93 (0.76-1.11)	< 0.0001
Maximum wall thickness (mm) ,median (IQR)	2.52 (1.99-3.64)	1.58 (1.23-2.0)	< 0.0001
Minimum wall thickness (mm) ,median (IQR)	0.51 (0.29-0.80)	0.40 (0.28-0.56)	0.276
WTI (mm²) , median (IQR)	94.38 (71.0-132.6)	39.12 (25.9-44.8)	< 0.0001
WTI% (%) , median (IQR)	27.01 (20.6-34.4)	27.09 (22.8-32.3)	0.85

Legend: IQR= interquartile range; SD= standard deviation; WTI= wall thickness index; WTI%= wall thickness index %.

Table 3. Comparison between pre and post ablation PV measurements in the ICE- and in the IVUS-imaged PVs.

	ICE imaged PVs		p	IVUS imaged PVs		p
	Pre-ablation	Post-ablation		Pre-ablation	Post-ablation	
Mean lumen diameter (mm), mean ± SD	18.57 ± 3.77	18.3 ± 3.97	0.557	10.96 ± 2.24	10.93 ± 2.16	0.893
Lumen area (mm2), mean ± SD	281.46 ± 115.06	275.48 ± 118.24	0.673	98.05 ± 36.74	97.36 ± 34.64	0.834
Mean vessel diameter (mm), mean ± SD	21.21 ± 3.72	21.54 ± 3.94	0.461	12.58 ± 2.5	12.95 ± 2.39	0.106
Vessel area (mm2), mean ± SD	363.84 ± 130.33	374.56 ± 139.38	0.523	129.02 ± 47.34	136.00 ± 46.33	0.126
Muscular sleeve thickness (mm), median (IQR)	0.55 (0.34-0.70)	0.37 (0.33-0.51)	0.001	0.35 (0.11-0.60)	0.22 (0.01-0.46)	0.034
Mean wall thickness (mm), median (IQR)	1.19 (0.95-1.52)	1.52 (1.21-1.9)	0.008	0.78 (0.67-0.84)	0.93 (0.76-1.11)	0.016
WTI (mm2), median (IQR)	73.39 (55.79 - 109.5)	94.38 (71.0 - 132.6)	0.006	29.67 (24.4 - 33.9)	39.12 (25.9 - 44.8)	0.006
WTI% (%), median (IQR)	22.18 (16.4 - 29.1)	27.01 (20.6 - 34.4)	0.012	23.15 (20.8 - 27.8)	27.09 (22.8 - 32.3)	0.0025

Legend: IQR= interquartile range; SD= standard deviation; WTI= wall thickness index; WTI%= wall thickness index %.

Table 5. Acute changes produced by catheter ablation: comparison among different PVI ablation energies.

	RF (18 PVs)	Cryo (15 PVs)	Laser (12 PVs)
Mean application time per vein	13.1 ± 2.1 min	1.9 ± 0.6 freezes (360 ± 95.5 sec)	19.5 ± 1.5 min
WTI% (%), median (IQR)			
Pre-ablation	21.21 (15.48 - 23.68)	25.06 (22.30 - 31.57)	25.30 (19.62- 29.93)
Post-ablation	25.83 (19.71- 31.39)	24.33 (20.45 – 32.02)	31.97 (26.92 – 36.98)
p	0.003	0.69	0.003
Muscular sleeve thickness (mm),median (IQR)			
Pre-ablation	0.36 (0.20- 0.64)	0.35 (0.01-0.56)	0.65 (0.45- 1.32)
Post-ablation	0.24 (0.02- 0.44)	0.25 (0.0-0.52)	0.39 (0.0- 0.55)
p	0.037	0.005	0.008

Legend: IQR= interquartile range; RF= radiofrequency energy; WTI% = Wall Thickness Index %.

Figures

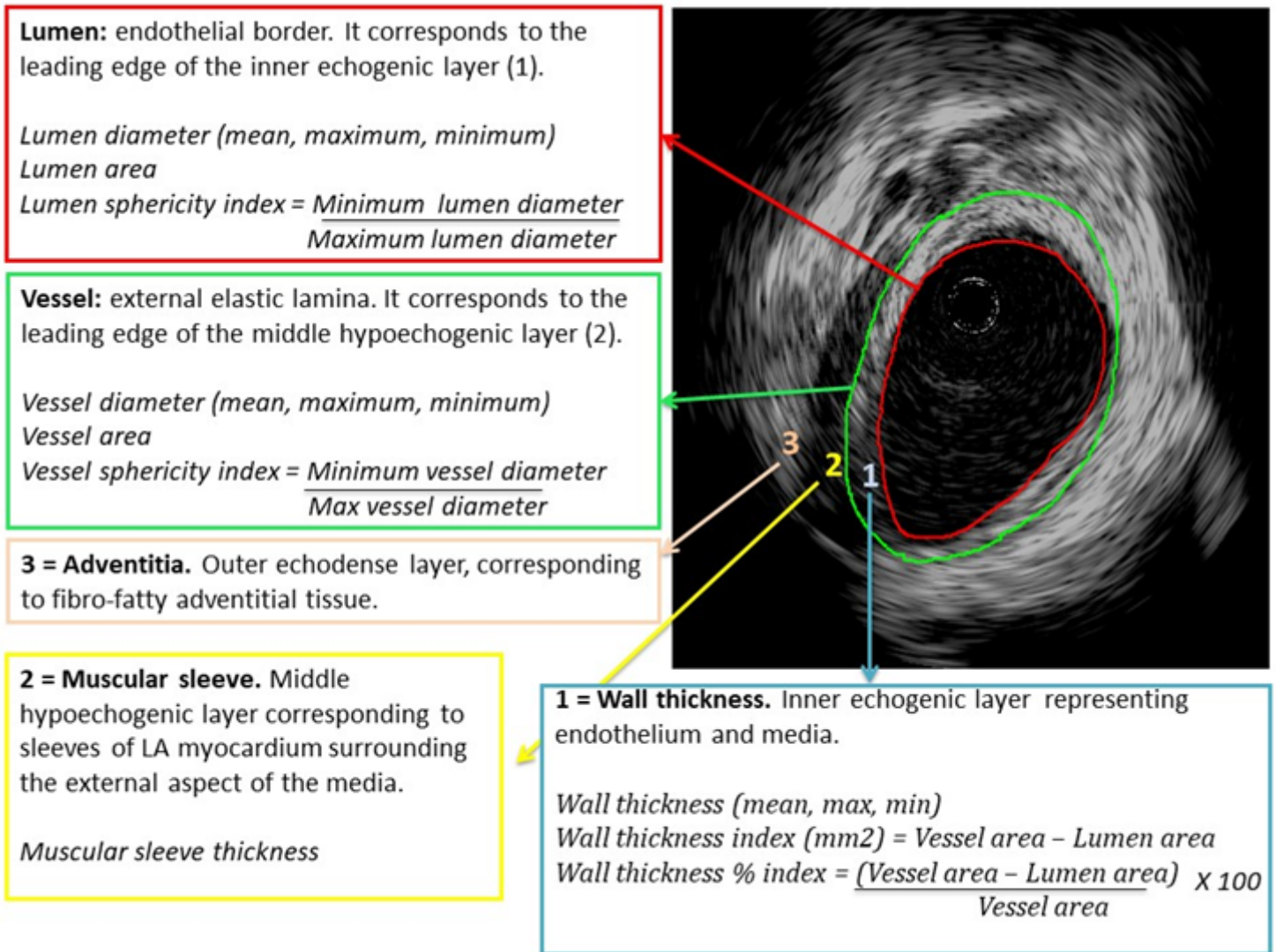


Figure 1

Analyses conducted on PV ostia frames: wall structures identified and measurements calculated (in italic).

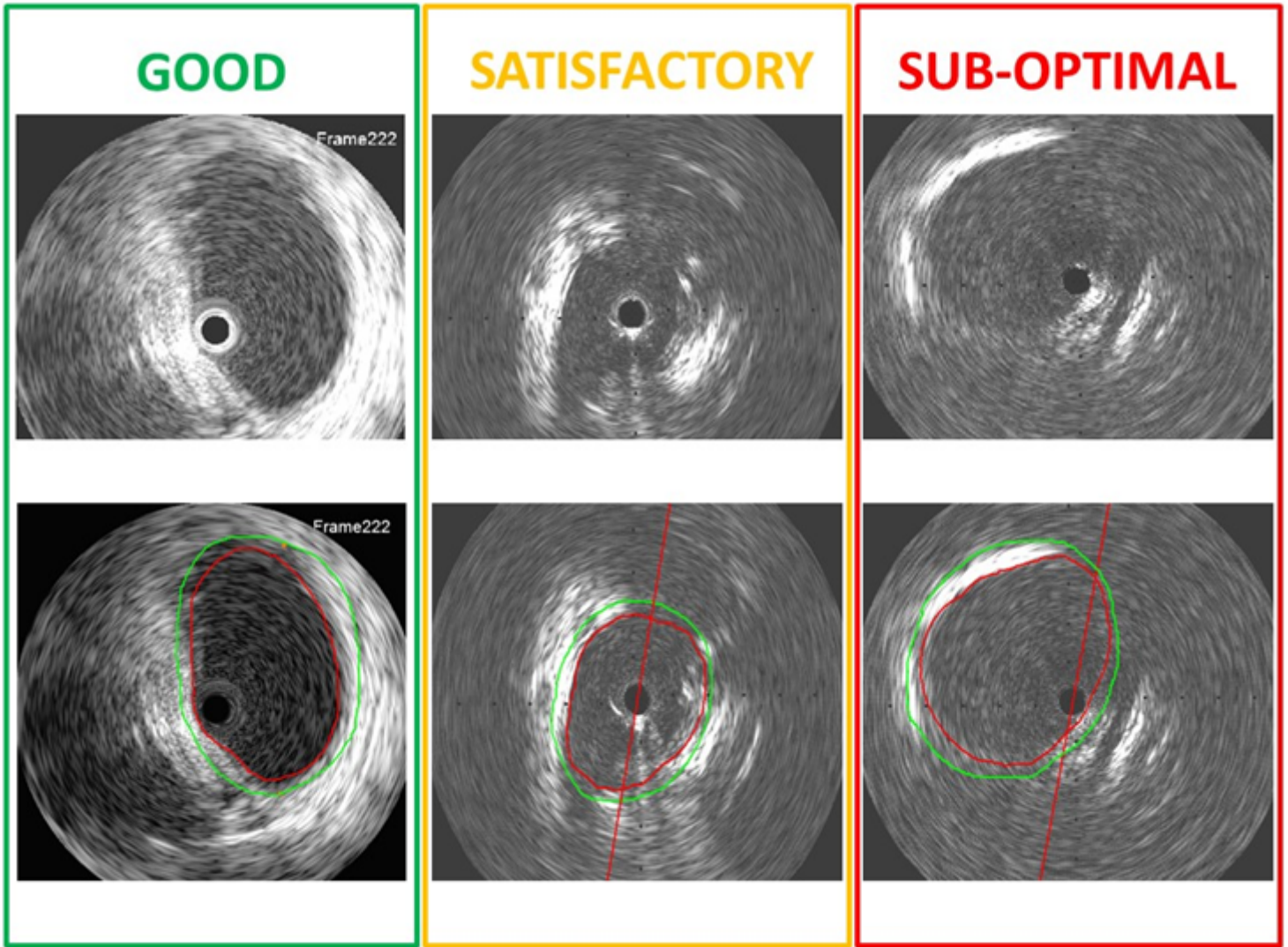


Figure 2

Grading of ICE/IVUS imaging quality, based on sharpness of the vessel contour in the 4 image quadrants. From left to right: examples of good quality, satisfactory quality and sub-optimal quality PV cross-sections.

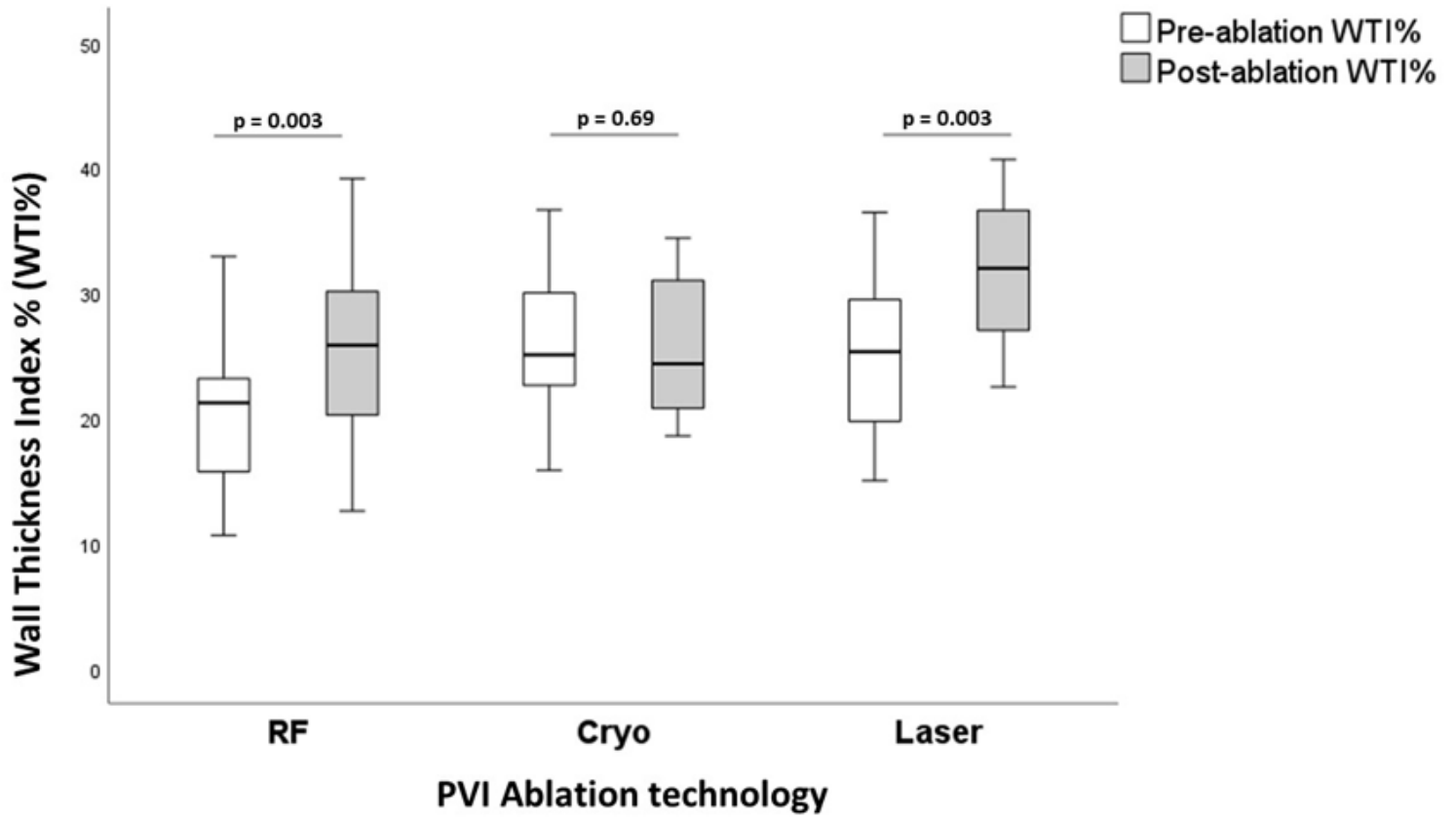


Figure 3

Wall thickness index % (WTI%) before and after ablation: comparison among different ablation energies for Pulmonary Vein Isolation (PVI).

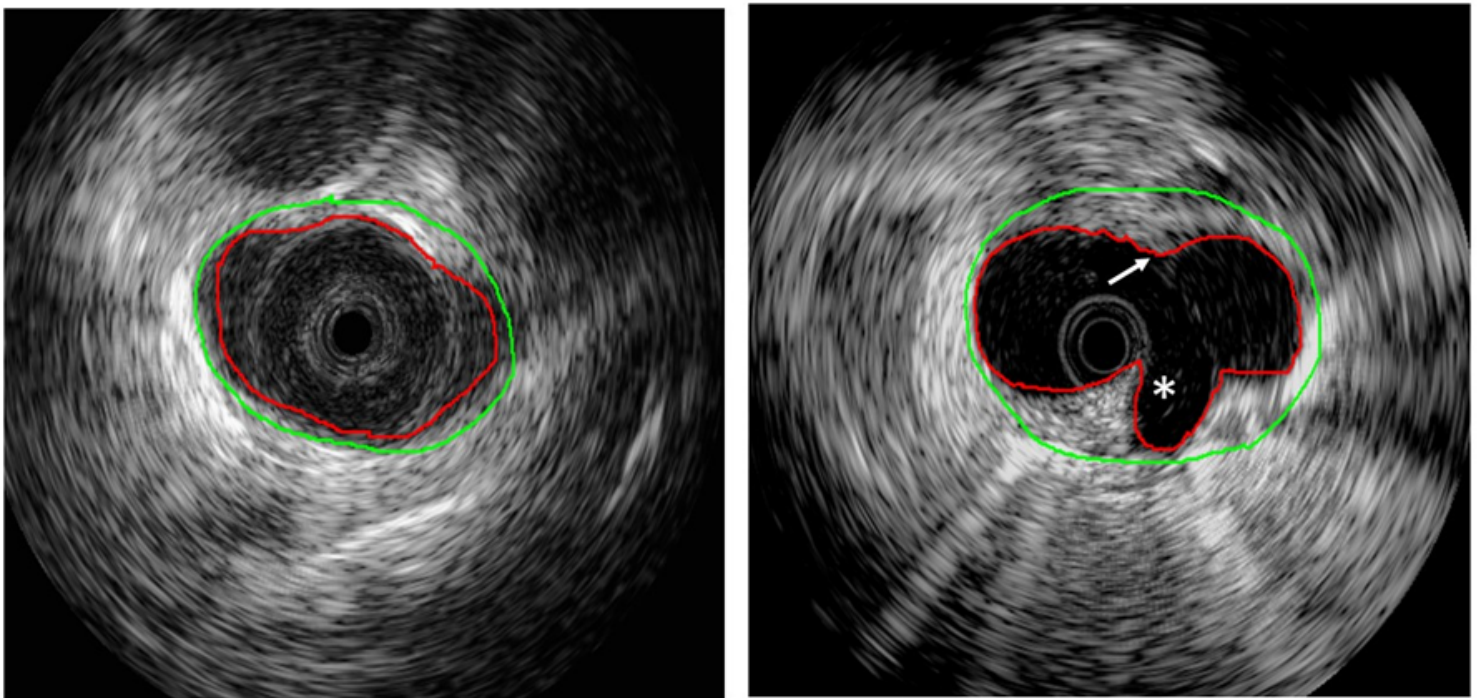


Figure 4

ICE image of ostium of same right inferior pulmonary vein, before (left panel) and after cryoablation (right panel). The white arrow indicates acute tissue thickening suggestive of oedema, while the white asterisk indicates a dissection flap.

Supplementary Files

This is a list of supplementary files associated with this preprint. Click to download.

- [Supplementarysection.docx](#)